Excitons in quantum boxes: Correlation effects and quantum confinement

Garnett W. Bryant
McDonnell Douglas Research Laboratories, P.O. Box 516, St. Louis, Missouri 63166-0516
(Received 11 December 1987)

Ultrasmall, quasi-zero-dimensional, quantum-box structures can now be made which exhibit quantum carrier confinement in all three dimensions. We present calculations of the properties of excitons confined in quantum boxes. The boxes are modeled as square (side L), flat plates (width w). Infinite barriers are used to confine the electron and hole. The effective-mass Schrödinger equation is solved to determine exciton properties. A variational wave function is used to calculate the exciton ground-state energy and optical properties. The exciton wave function is also expanded in terms of electron-hole configurations made from electron and hole single-particle box states. This wave function is used to study the onset of correlation effects. Exciton ground-state total energies, interaction energies, Coulomb energies, kinetic energies, electron-hole separations, and oscillator strengths are determined. The results illustrate the competing effects of quantum confinement and Coulomb-induced electron-hole correlations. For large boxes ($L \gtrsim 100$ nm) excitons in quantum boxes are strongly correlated and confinement effects are negligible. In small boxes ($L \lesssim 10$ nm) excitons are weakly correlated. Confinement effects are dominant and the electron and hole occupy the lowest-energy pair of single-particle levels. Confinement enhances the exciton kinetic and direct Coulomb energies, reduces the electron-hole separation, and increases the oscillator strength. Even in the transition regime (10 nm $\lesssim L \lesssim 100$ nm), the enhancement of exciton oscillator strengths could enhance optoelectronic properties.

I. INTRODUCTION

The optical properties of quasi-two-dimensional semiconductor single- and multiple-quantum-well (QW) systems have been studied intensely to determine how quantum confinement in the well affects the electronic states and band structure of QW systems. The elementary optical excitations created by photons near an absorption edge are excitons. The fundamental effects of quantum confinement on excitons in quasi-two-dimensional QW systems are now well known. The degeneracy of the light-hole and the heavy-hole bands is lifted by the confinement and both light- and heavy-hole excitons can exist. The interaction between confined electrons and holes is more effective than the bulk electron-hole interaction and the confined-exciton binding energy is enhanced. With the recent advances in the art of microfabrication, quantum microstructures can now be made which exhibit quantum carrier confinement in two dimensions [quantum well wires (QWW)[1-6]] and in all three dimensions [quantum boxes (QB)[2-7] and microcrystallites[8-11]]. These structures provide new systems for the study of quantum-confinement effects.

In this paper we investigate the nature of excitons in quantum boxes. Quantum-confinement effects should be most severe for systems confined in all dimensions. In a QW or QWW the spectrum of single-particle states is a set of subbands of two- or one-dimensional states, respectively (see Fig. 1). Each subband is a continuum of states. The separation between subbands is determined by the splitting between the levels for the confined motion. Although this splitting increases as the strength of the confinement increases (the well size decreases or the barrier height increases), there is always a continuum of states which can be mixed to account for the electron-hole correlation in the exciton. In a quasi-zero-dimensional structure with confinement in all directions, the density of states is a set of discrete states. The level-splitting scales as $1/L^2$ while the electron-hole attraction responsible for mixing single-particle state scales only as $1/L$ when the scale of confinement L is varied. Thus, as the confinement in a quasi-zero-dimensional structure increases, the mixing of states needed to account for electron-hole correlation in the exciton becomes more difficult, and the electron and hole become frozen in the lowest-energy single-particle states. Freeze out of motion in the confined dimension also occurs in QW and QWW when the confinement is increased, but correlation of the unconfined motion in a QW or QWW is enhanced by the greater overlap of the confined electron-hole pair. In a zero-dimensional structure all motion is confined, so confinement should weaken correlations of all motion.

In this paper we focus our attention on excitons in quasi-zero-dimensional structures in part because such excitons have not been studied extensively. Typical quasi-zero-dimensional structures are semiconductor microcrystallites[8-11] prepared in colloidal form or embedded in optical glasses and semiconductor quantum boxes[2-7] fabricated by lateral confinement of quasi-two-dimensional quantum wells by implantation-enhanced interdiffusion[2,3] or by electron-beam lithography.[4-7] The microcrystallites are approximately spherical in shape, and motion is three-dimensional inside the structure. In contrast, quantum boxes are thin disks with the two dimensions defined by lateral confinement much larger than the width of the quantum well that defines the third di-

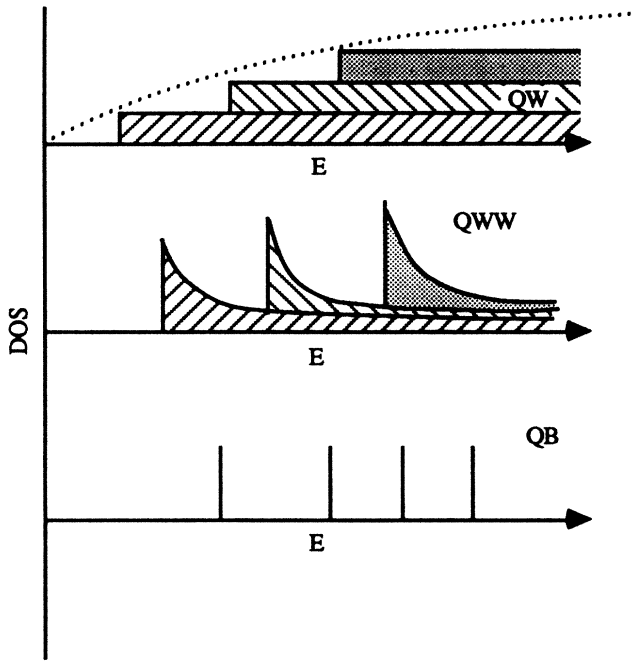

FIG. 1. The electronic density of states (DOS) for systems confined in one (quantum well), two (quantum-well wire) and three (quantum box) dimensions. The dashed line is the DOS for a bulk system.

mension of the box (see Fig. 2). The internal motion is quasi-two-dimensional. The theoretical understanding of excitons in microcrystallites is being developed.[8,11–16] However, the theoretical description for excitons in QB's has not been developed to the same extent.[17,18] For that reason, we restrict our attention to excitons in QB's.

The qualitative effects of confinement on excitons is the same for excitons in microcrystallites and QB's. An exciton in a large QB (microcrystallite) behaves as a free, quasi-two- (three-) dimensional exciton. As the size L of the box or microcrystallite decreases, confinement effects become important. For very small L the exciton is quasi-zero-dimensional with all motion frozen out. However, confinement effects in microcrystallites and QB's should differ quantitatively because one degree of motion is frozen out in QB's for all L. In this paper we determine the length scale on which the transition from negligible to complete confinement occurs for excitons in quantum boxes and how the transition is manifested by changes in exciton ground-state energies, radius, and optical absorption. The results will be used to gain additional understanding of recent photoluminescence (PL) experiments in which excitons were observed in quantum boxes[4–7] and to determine whether excitons in presently fabricated boxes ($L \sim 30$–100 nm) really are confined. Recently, it has been suggested that the complete confinement of excitons in sufficiently small quantum boxes will enhance the optical properties of excitons enough that QB's may find applications in laser structures[19] and in devices utilizing optical bistability.[20] Our results will be used to determine how complete the confinement must be before optical properties are enhanced. The theoretical model used to describe excitons in quantum boxes is discussed in Sec. II, results are presented in Sec. III, and conclusions are made in Sec. IV.

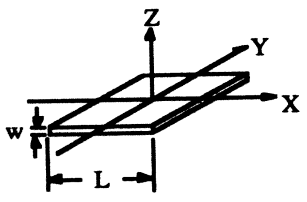

FIG. 2. The configuration of a quantum box.

II. THEORY

Microfabricated quantum boxes are constructed from narrow, two-dimensional quantum wells by processing the wells to laterally confine the two-dimensional motion. Typically, the width w of the two-dimensional quantum well is an order of magnitude less than the length L of the side of the box, so the box is a thin plate or disk. We model the quantum boxes as square plates with sides of length L and width w. Such a quantum box is shown in Fig. 2. Fabricated quantum boxes are typically circular rather than square. However, shape effects are minimal for structures with the same cross-sectional area.[21] For example, the properties of an exciton confined in a circular disk of radius R should be nearly the same as the properties of an exciton in a square plate with side $L = \sqrt{\pi} R$.

The exciton states are determined by solving the electron-hole effective-mass Schrödinger equation. The electron-hole interaction is the Coulomb interaction screened by the background dielectric constant ϵ. Polarization and image charge effects can be significant when there is a large dielectric discontinuity between the quantum box and the surrounding medium.[16] This is not the case for microfabricated boxes made, for example, with GaAs wells and AlGaAs barriers; therefore, we ignore such effects.

The effective-mass Hamiltonian is

$$H = \sum_{i=e,h} \left[-\frac{\hbar^2}{2m_{\parallel,i}} \left(\frac{d^2}{dx^2} + \frac{d^2}{dy^2} \right) - \frac{\hbar^2}{2m_{\perp,i}} \frac{d^2}{dz^2} + V_i \right] - \frac{e^2}{\epsilon \, | \mathbf{r}_e - \mathbf{r}_h |} , \tag{1}$$

$$V_i = \begin{cases} 0 & \text{if } |x_i|, |y_i| < L/2 \text{ and } |z_i| < w/2 \\ \infty & \text{otherwise} . \end{cases} \tag{2}$$

The effective mass in the plane of the disk $m_{\parallel,i}$ is assumed to be isotropic, but it need not be the same as the mass $m_{\perp,i}$ for motion perpendicular to the plane. An infinite barrier is used to confine the exciton in the box.

Real barriers are finite. However, a good model for the barriers which define the edge of the disk does not exist yet. Although carriers can tunnel from boxes with finite barriers, this tunneling does not change the electronic properties qualitatively until $L \lesssim 5$ nm.[22] Calculations are greatly simplified by use of the infinite-barrier model. The x, y, and z motions for the single-particle states in an infinite-barrier square plate are separable. The single-particle states are products of the simple one-dimensional-particle-in-an-infinite-well states (sines and cosines).

Two approaches have been used to solve Eq. (1). First, accurate ground states for confined excitons have been calculated by use of a variational approach. The exciton variational wave function Ψ is chosen to be a product of the electron and hole lowest-energy subband states and a linear combination s of Gaussian functions of the electron-hole separation to account for correlation in the exciton

$$\Psi(\mathbf{r}_e,\mathbf{r}_h)=c(\mathbf{r}_e)c(\mathbf{r}_h)s(\mathbf{r}_e,\mathbf{r}_h)\ , \tag{3a}$$

$$\frac{c(\mathbf{r}_i)=\cos(kx_i)\cos(ky_i)\cos(qz_i)}{\sqrt{L/2}\sqrt{L/2}\sqrt{w/2}}\ , \tag{3b}$$

$$s(\mathbf{r}_e,\mathbf{r}_h)=\sum_n c_n \exp\{-\alpha_n[(x_e-x_h)^2+(y_e-y_h)^2]\} \tag{3c}$$

with $k=\pi/L$, $q=\pi/w$. Accurate energies and wave functions are obtained by use of 5 to 10 Gaussians. No correlation function of z_e and z_h has been included. Typical well widths w are less than 5 nm and the energy levels in the well are sufficiently separated that the electron and hole occupy the lowest-energy well states. The single-subband approximation for confined motion gives good results for quantum wells,[23] quantum-well wires,[22] and quantum boxes (see Sec. III) when $L \lesssim 5$ nm.

The form chosen for Ψ gives the correct results for the ground state of the exciton in the limits of complete (small L) and negligible (large L) confinement. In the small-L limit $s(\mathbf{r}_e,\mathbf{r}_h)\equiv 1$. In the large-$L$ limit $s(\mathbf{r}_e,\mathbf{r}_h)$ is the bulk-exciton ground-state wave function, and $c(\mathbf{r}_e)$ and $c(\mathbf{r}_h)$ are envelope functions which are slowly varying on the scale of the exciton. Consequently Eq. (3) should provide an adequate interpolation between the large- and small-L limits. This is especially true when the electron and hole masses are similar because the electron and hole are treated equivalently in Eq. (3). When the electron and hole masses are very different a more complicated variational function should be used. For example, when the hole mass is much heavier than the electron mass,[12] the hole is more strongly localized than the electron for L in the transition regime between negligible and complete confinement, and the wave function must account for this effect. The lowest-energy exciton in a box constructed from a GaAs well and AlGaAs barriers is made with a hole which has a light in-plane mass similar to the electron mass and a heavy mass in the perpendicular direction. Equation (3) should be a good wave function for this exciton. We also consider excitons constructed from a hole with a heavy in-plane mass and a light perpendicular mass. In this case, Eq. (3) will be less reliable for L in the transition region. However, we have not yet tried more complicated forms for Ψ. Exciton excited states could also be described with variational wave functions. We have not attempted to model any excited states by use of a variational approach.

A configuration-interaction approach[24] has also been used to calculate exciton states. The electron-hole wave function is expanded in terms of products of the electron and hole single-particle, noninteracting eigenstates. The kinetic energy and interaction matrix elements[21] are found using this basis, and the Hamiltonian is diagonalized to find the eigenstates. The number of basis functions included in the expansion is increased until the desired accuracy is achieved. In very small boxes, the electron and hole are frozen in the lowest single-particle levels and are uncorrelated. As L increases, the electron and hole become correlated and higher energy levels are mixed into the exciton ground state. The CI approach is ideal for studying the onset and evolution of the electron-hole correlation as L increases because the mixing of higher-energy states is explicitly included.

Using the exciton variational wave function, we also calculate the electron-hole separation R in the plane of the disk and the exciton ground-state oscillator strength f. For R we calculate

$$R=\langle(x_e-x_h)^2+(y_e-y_h)^2\rangle^{1/2}\ , \tag{4}$$

where the brackets denote the expectation value in the exciton ground state. Since we assume that the well width w is small and the electron and hole are confined to the lowest z subbands, $\langle(z_e-z_h)^2\rangle$ is a function only of w and does not change as the quantum confinement (L) changes.

For a multielectron system one can derive[25] the following f sum rule:

$$\sum_s f_{s,t}=N_e\ , \tag{5}$$

where

$$f_{s,t}=\frac{2\left|\left\langle s\left|\sum_i p_{x_i}\right|t\right\rangle\right|^2}{m(E_s-E_t)}\ . \tag{6}$$

The sum in Eq. (5) is over all states of the system, N_e is the number of electrons, m is the electron mass and the sum in Eq. (6) is the sum over all electrons.

The oscillator strength for the exciton ground state is

$$f_{\rm ex}=\frac{2}{m}\frac{\left|\left\langle \mathrm{ex}\left|\sum_i p_{x_i}\right|0\right\rangle\right|^2}{E_{\rm ex}-E_0} \tag{7}$$

where $|\mathrm{ex}\rangle$ and $|0\rangle$ are the states with and without the exciton. Using the envelope-function approximation, one can derive[26]

$$f_{\rm ex}=\frac{2P^2}{m(E_{\rm ex}-E_0)}\left|\int \Psi_{\rm ex}(\mathbf{r}_e,\mathbf{r}_e)d^3r_e\right|^2\ , \tag{8}$$

where P includes all intracell matrix-element effects, $\Psi_{\rm ex}$ is the exciton envelope function given, for example, by Eq. (3) with the electron and hole at the same position. If

Ψ_{ex} is normalized as one exciton per quantum box in Eq. (8), then N_e [Eq. (5)] is the number of electrons in the box. This expression has been derived previously[26] for the oscillator strength of exciton bound to neutral donors and acceptors. Equation (8) also reduces to the oscillator strength of a free exciton if $\Psi_{ex}(\mathbf{r}_e,\mathbf{r}_e)$ is independent of $\mathbf{r}_e$.

All of the calculations have been performed with the assumption that the boxes are GaAs wells. Since infinite barriers are used, the results are independent of the parameters of the barrier. The GaAs parameters used are $\epsilon=13.1$; $m_{\perp e}=m_{\parallel e}=0.067m$; for light holes $m_{\perp h}=0.09m$, $m_{\parallel h}=0.377m$; and for heavy holes $m_{\perp h}=0.377m$, $m_{\parallel h}=0.09m$. Energies are scaled by electron effective Rydberg $R_e=e^2m_e/2a_0^2\epsilon^2=5.3$ meV. No attempt has been made to model matrix-element effects included in P. However, to obtain the correct order of magnitude for f we use $P^2/m=1$ eV, which is typical for III-V semiconductors.[27]

III. RESULTS

Calculations have been performed for excitons in quantum boxes made from wells with $w=0$, 2, and 5 nm. We present results for excitons in two-dimensional boxes ($w=0$) first to illustrate qualitatively the effects of quantum confinement as L is varied. We then present results for excitons in quasi-two-dimensional boxes ($w=2$ and 5 nm) to show quantitatively the changes which occur when the box has a finite-well width.

The ground-state energy E_{GS} of the confined heavy-hole (light in-plane mass and heavy perpendicular mass) exciton in a square, two-dimensional ($w=0$) box is shown in Fig. 3. Since $w=0$, no confinement energy due to perpendicular motion is included. The results were obtained using the variational wave function. For small L, accurate energies can also be obtained by the CI approach and these energies agree with energies obtained variationally. Equation (3) should be most appropriate for the heavy-hole exciton because the in-plane hole mass and the electron mass are similar. The CI calculations confirm that the electron and hole in the heavy-hole exciton can be treated equivalently, as in Eq. (3), because the electron and hole parts of the wave function determined by the CI calculations are almost the same.

At small L the confinement energy increases as $1/L^2$, and the interaction energy increases as $1/L$. The confinement energy dominates, and the ground-state energy increases monotonically with decreasing L. Similar results have been obtained in calculations for microcrystallites.[12–16] At large L ($L\gtrsim 100$ nm), the exciton ground-state energy approaches the energy for the unconfined, two-dimensional exciton [$-4R_\mu$, where R_μ is the exciton (reduced-mass μ) effective Rydberg]. The shift from the limiting value is less than 5% for $L\gtrsim 100$ nm.

There are two ways to split the ground-state energy to illustrate the effects of quantum confinement:

$$E_{GS}=E_{NI}+E_I\ , \tag{9}$$

$$E_{GS}=E_{KE}+E_C\ . \tag{10}$$

E_{NI} is the energy of an uncorrelated, noninteracting, electron-hole pair confined in the lowest-energy quantum-box states. E_I is the shift in exciton energy that occurs when the interactions are included. E_{KE} and E_C are the kinetic and Coulomb energies for the exciton. Furthermore, E_I and E_C are related by

$$E_I=E_C+\Delta E_{KE}\ , \tag{11}$$

where ΔE_{KE} is the change in kinetic energy which occurs when a noninteracting electron-hole pair become correlated by the interactions. These energies are shown in Fig. 3. The confinement energy E_{NI} displays the most rapid variation as L decreases. This would suggest that confinement effects are important even for $L\gtrsim 100$ nm. However, for these L, the exciton is much smaller than the box, and the exciton ground-state energy E_{GS} is affected little by confinement. The exciton kinetic and Coulomb energies show a similar weak dependence on L for larger boxes. In fact E_{KE} is much larger than E_{NI} for

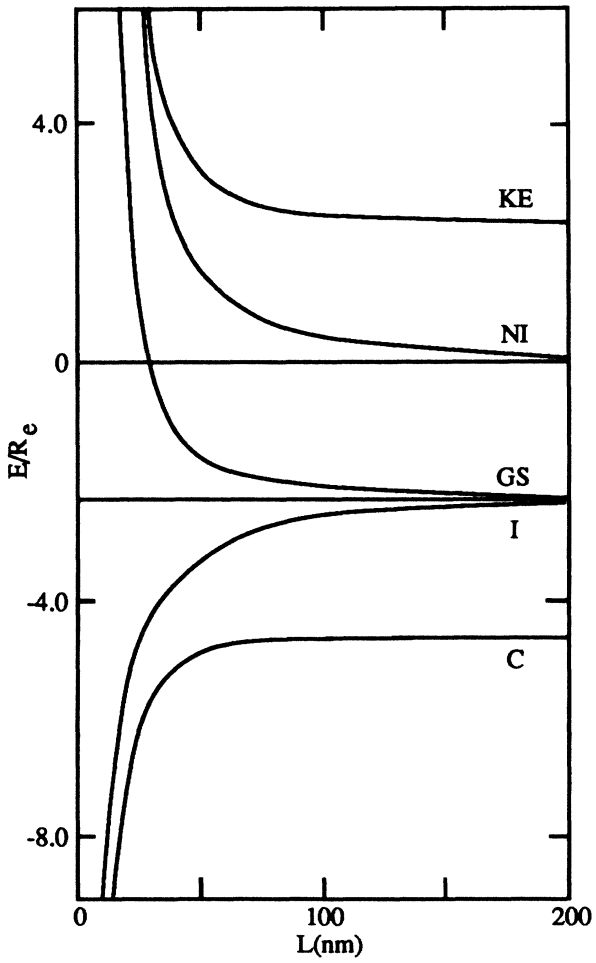

FIG. 3. The ground-state (GS) energy of an exciton confined in a square box with sides of length L. The exciton kinetic energy (KE) and Coulomb energy (C), the energy of a noninteracting electron-hole pair (NI), and the interaction energy (I) are shown. For these results $w=0$, $m_{\parallel,h}=0.09m$, and $m_{\perp,h}=0.377m$.

large L. Most of the kinetic energy of an exciton in a large box is the kinetic energy due to correlation as an exciton, and only a small part is due to quantum confinement. As L decreases, E_{KE} increases more rapidly than E_C, indicating that the kinetic-energy effects are more sensitive to confinement than are Coulomb interactions. Moreover, as L decreases, E_{KE} approaches E_{NI}, indicating that the correlation effects in the exciton due to the interactions are becoming less important and that quantum confinement makes the more important contribution.

Recently, Wu *et al.*[18] showed that the broad photoluminescence peaks observed for excitons in quantum boxes[4–6] could result from inhomogeneous broadening due to variations in box size because the exciton energy was a sensitive function of L. For the exciton energy they used E_{NI}, which varies as $1/L^2$. Our results show that the actual exciton energy E_{GS} is much less sensitive to L. For $L \gtrsim 100$ nm, E_{GS} is almost constant; and for 30 nm $\lesssim L \lesssim 100$ nm, E_{GS} changes more slowly than E_{NI} by a factor of 2 or more. Inhomogeneous line broadening should not affect peak widths as much as suggested by Wu *et al.* because $L \gtrsim 30$ nm for boxes currently being fabricated.

The ground-state and interaction energies for confined, two-dimensional ($w=0$) excitons with in-plane hole masses $m_{\|h}=0.090m$ and $0.377m$ are compared in Fig. 4.

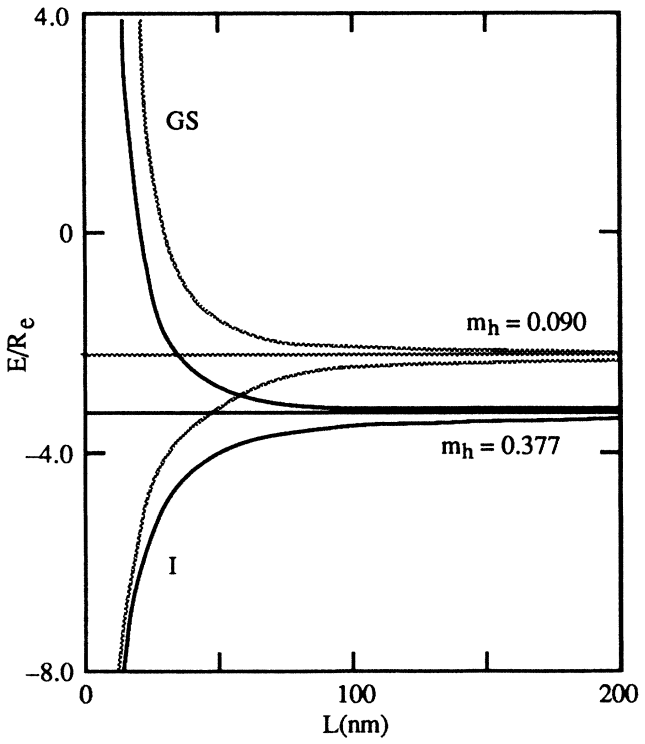

FIG. 4. The ground-state (GS) and interaction (I) energies for confined, two-dimensional ($w=0$) excitons with in-plane masses $m_{\|,h}=0.090m$ and $m_{\|,h}=0.377m$ as indicated. The horizontal curves give the limiting values for free two-dimensional excitons.

Coulomb effects are weaker, and quantum confinement occurs at larger L for the heavy-hole exciton because this exciton is formed from a hole with a light in-plane mass. The confined, two-dimensional ($w=0$), heavy-hole exciton has a higher ground-state energy than the light-hole exciton. However, when $w\neq 0$ and the confinement energy for perpendicular motion is included, the heavy-hole exciton has the lower ground-state energy.

As L decreases and confinement effects become dominant, the splitting between the quantum-box single particle states becomes large, and the electron and hole in the exciton become increasingly confined to the lowest-energy well states. In the limit of complete quantum confinement, the interaction effects would be independent of hole mass, because the hole would occupy only the lowest-energy state and thus would have a wave function which was independent of hole mass. From Fig. 4, it is clear that the onset of complete quantum confinement occurs for $L \lesssim 10$ nm, where E_I becomes insensitive to $m_{\|,h}$.

One might expect the onset of quantum-confinement effects to occur when the size of the exciton is comparable to the size of the box. One might also expect the onset of quantum-confinement effects to occur when the splitting ΔE_{NI} between the ground state for a noninteracting pair and the first excited state that can mix with the ground state is comparable to E_I. The electron-hole separation [as defined in Eq. (4)] for a free, two-dimensional exciton is

$$a^{2D}=\sqrt{3/8}\epsilon a_0/\mu ,$$

where a_0 is the Bohr radius and μ the exciton reduced mass. For $m_{\|,h}=0.090m$, $a^{2D}=10.9$ nm; and for $m_{\|,h}=0.377m$, $a^{2D}=7.46$ nm. Thus the exciton radius is an order of magnitude smaller than L (~ 100 nm), where confinement effects begin. In fact, the transition to complete confinement occurs ($L \sim 10$ nm) when the length of the box is comparable to the free-exciton radius. The ratio of interaction energy to level splitting $E_I/\Delta E_{NI}$ gives a more accurate criterion for the onset of confinement effects. For $m_{\|,h}=0.090m$, $E_I/\Delta E_{NI}=1$ when $L=65$ nm; for $m_{\|,h}=0.377m$, $E_I/\Delta E_{NI}=1$ when $L=36$ nm (see Fig. 5). Thus the level spacing becomes comparable to the interaction energy for L in the middle of the transition region from negligible ($L \lesssim 100$ nm) to complete confinement ($L \lesssim 10$ nm). Furthermore, the shift of this transition to lower L for the exciton with the heavier in-plane mass is consistent with the shift of the value for L where $E_I/\Delta E_{NI}=1$.

In a two-dimensional ($w=0$) quantum box the electron-hole interaction has the Coulomb singularity. In a quantum box with a finite thickness ($w\neq 0$) the effective, two-dimensional, electron-hole interaction is weakened because the singularity is cutoff by the smearing of the wave function in the z direction. This weakening of the effective electron-hole interaction changes the exciton energies quantitatively but not qualitatively. Figure 6 shows the change in interaction energy $\Delta E_I=E_I(w)-E_I(w=0)$ that occurs for a box with a finite w. (The exciton energy for $w\neq 0$ would also include

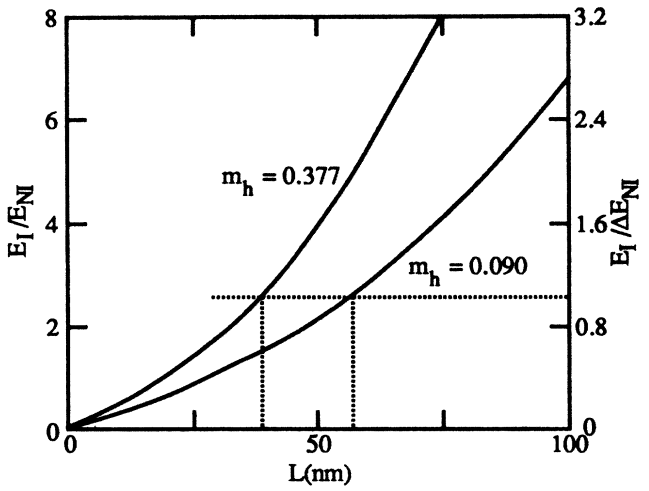

FIG. 5. E_I/E_{NI} and $E_I/\Delta E_{NI}$ for confined two-dimensional ($w=0$) excitons.

the confinement energy for the z direction.) As expected, the shifts are larger for excitons with heavy in-plane holes and for thicker wells. More importantly, ΔE_I is independent of L for large boxes ($L \gtrsim 50$ nm), and ΔE_I becomes independent of $m_{\perp,h}$ for $L \lesssim 10$ nm (the onset of complete confinement). E_{GS} ($w \neq 0$) has the same sensitivity to box confinement as E_{GS} ($w=0$). Thus the effects of box confinement should be qualitatively the same independent of w. The calculations were performed by using infinite barriers to define the confinement in the z direction. Finite barriers appropriate for the band discontinuity between GaAs and $Al_xGa_{1-x}As$ should be used. However, the effects of a finite barrier can be modeled by use of a wider well with an infinite barrier. Little qualitative change in exciton energies would occur in a finite-barrier model since the qualitative behavior of the energies is independent of w in the infinite-barrier model.

In the limit of very small boxes, the splitting between noninteracting pair levels becomes very large, and the electron-hole pair is confined to the lowest-energy state. In this limit the direct Coulomb energy makes the dominant contribution to E_I. In Fig. 7 the interaction energy, E_I^{1sb} found in the approximation of complete quantum confinement with the electron-hole pair in the lowest-energy state and denoted the one-subband approximation, is compared with E_I found with Eq. (3). The one-subband approximation gives 90% of the interaction energy for $L \lesssim 10$ nm. The accuracy is better when the interactions are weaker (i.e., for large w or light in-plane hole mass).

For two-dimensional ($w=0$) excitons, $E_I^{1sb}/E_I \approx 1 - CL$ for small L. Since $E_I^{1sb} \sim 1/L$, $E_I = E_I^{1sb} + C'$ at small L. Thus there is a finite shift between E_I and E_I^{1sb} due to correlation that occurs as a contribution from second-order perturbation theory even for very small L. Our results suggest that $C' \approx 1.2\, R_\mu$, where R_μ is the excitonic effective Rydberg. For boxes with wells of finite thickness ($w \neq 0$), the singularity in the effective interaction is cut off, $E_I^{1sb}/E_I \approx 1 - CL^2$ for small L, and the second-order contribution due to correlation vanishes for small L. If we define the correlation energy to be $E^{cor} = E_I - E_I^{1sb}$ then Fig. 7 shows that less than 10% of E_I is due to correlation for $L \lesssim 10$ nm, but more than half of E_I is due to correlation for $L \gtrsim 50$ nm.

The probability P_1 that the exciton is in the uncorrelated, lowest-energy pair state is shown in Table I for a

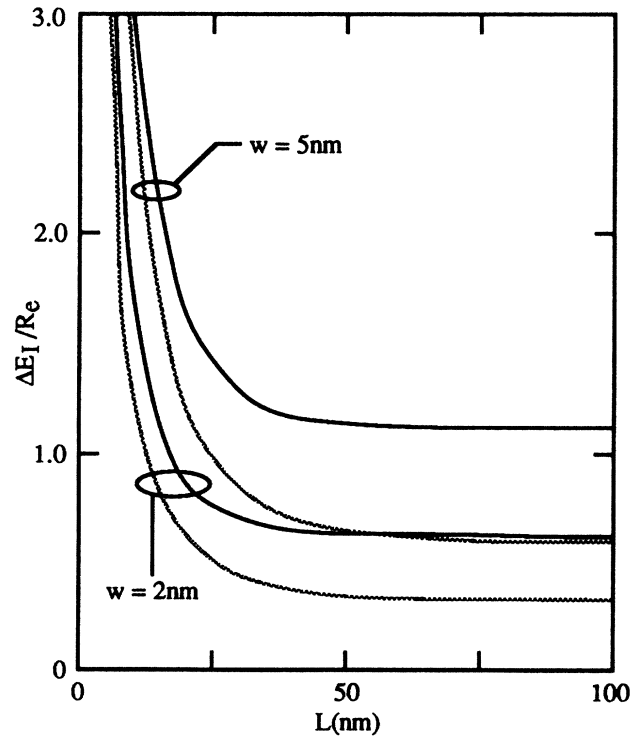

FIG. 6. Shift of the exciton interaction energy ΔE_I for $w=2$ and 5 nm. The solid curves are for the light-hole exciton ($m_{\perp h}=0.09m$, $m_{\parallel h}=0.377m$); the dashed curves are for the heavy-hole exciton.

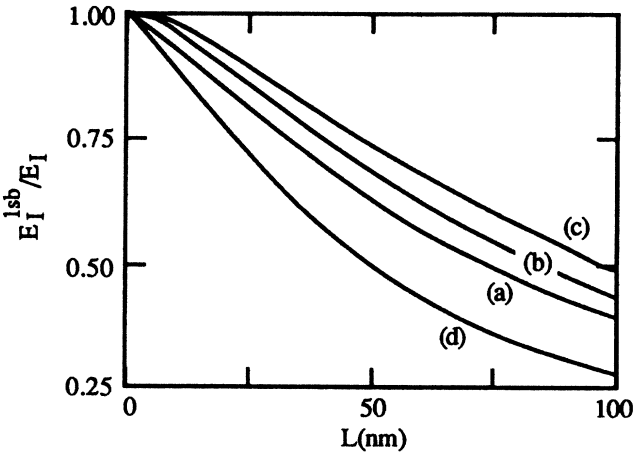

FIG. 7. One-subband approximation for the confined-exciton interaction energy: for an exciton with $m_{\parallel,h}=0.09m$ and $m_{\perp,h}=0.377m$, (a) $w=0$, (b) $w=2$ nm, and (c) $w=5$ nm; and (d) for the light-hole, two-dimensional ($w=0$) exciton.

TABLE I. Contribution of higher subbands to the interaction energy of a confined two-dimensional exciton with light in-plane hole mass. E_I^{nsb} is the interaction energy found by use of n electron and n hole subbands; E_I is the interaction energy determined with a variational wave function. P_1 is the probability that the electron-hole pair is in the lowest-energy pair state, calculated by use of $n=6$.

	E_I^{nsb}/E_I				
L (nm)	1	2	4	6	P_1
5	0.960	0.979	0.996	0.999	0.997
10	0.921	0.956	0.991	0.997	0.988
20	0.837	0.902	0.972	0.989	0.950
60	0.544	0.665	0.824	0.899	0.641
100		0.491	0.666	0.773	0.413

confined two-dimensional exciton with light, in-plane hole mass. Correlation effects must be included to obtain accurate E_I even in the limit of complete quantum confinement ($P_1 \approx 1$). These correlation effects can be added perturbatively by going beyond the one-subband approximation for the exciton wave function. Table I shows the interaction energy E_I^{nsb} calculated by use of n ($n=1,2,4$, and 6) electron and n hole subbands. When $L \lesssim 10$ nm, use of six subbands in a wave-function expansion accounts for almost all of the correlation energy. For $L \gtrsim 50$ nm, higher subbands must be included to obtain accurate correlation energies. Correlation in the wave function is even more important for properties which are more sensitive to the wave function. For example, use of six subbands does not provide an accurate oscillator strength because the oscillator strength is sensitive to the exciton wave function evaluated for vanishing electron-hole separation.

The electron-hole separation R for confined two-dimensional excitons is shown in Fig. 8. For $L \gtrsim 100$ nm, R is unaffected by the confinement. For $L \lesssim 10$ nm, R approaches the value expected in the limit of complete confinement. The onset of confinement effects and the transition to complete confinement determined by the behavior of R are the same as obtained from the behavior of the ground-state energy. R for an exciton with a light in-plane hole mass has also been calculated by use of only the part s of the exciton wave function due to correlations. For large L, s is the same as the bulk-exciton wave function. As L decreases, correlations become less important, and the value of R determined with a wave function which contains the correlation effects but no confinement effects actually increases. Box confinement rather than correlation effects shrink the exciton as L decreases. When the well has finite thickness ($w \neq 0$), the effective Coulomb interaction is weaker so R is larger. However, as with the E_{GS}, R does not change qualitatively (see Fig. 9) when $w \neq 0$. The transition from negligible confinement and the onset of complete confinement are insensitive to w.

Oscillator strengths for excitons with light in-plane hole mass are shown in Fig. 10. The exciton oscillator strength depends on the integral of $\Psi(\mathbf{r}_e,\mathbf{r}_e)$ and on an energy denominator [see Eq. (8)]. For small L, the exci-

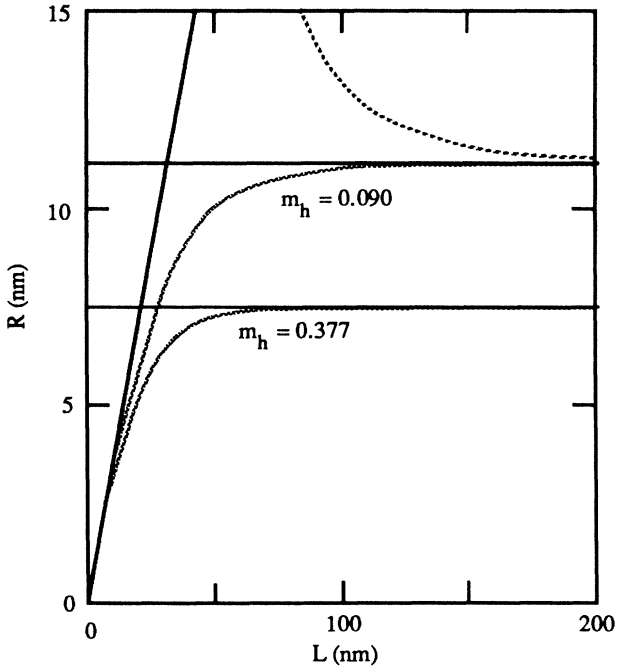

FIG. 8. Electron-hole separation R of a confined, two-dimensional ($w=0$) exciton in a square box. The horizontal solid lines indicate R for unconfined excitons with the indicated in-plane hole mass. The other solid curve is R calculated for an uncorrelated electron-hole pair confined to the lowest pair of subband states. The dashed curves that interpolate between the solid lines are the R for the exciton states. The upper dashed curve is R for $m_h = 0.090m$ calculated by use of only the correlated part s of the exciton wave function.

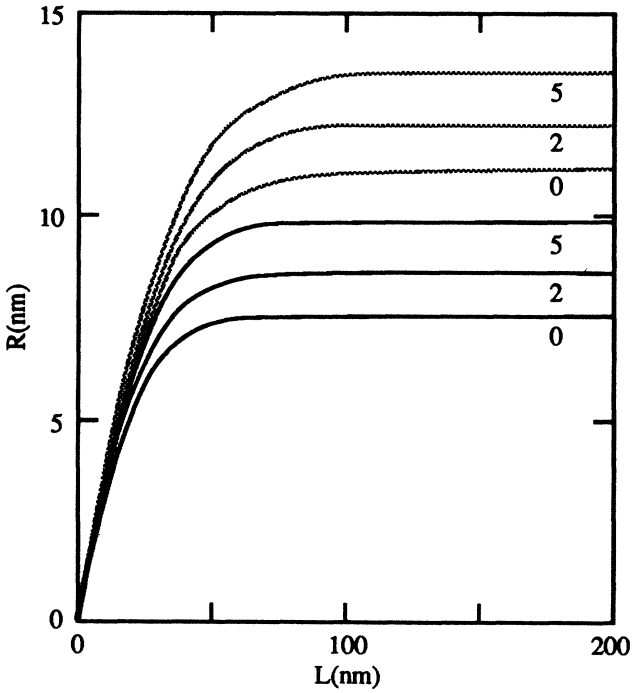

FIG. 9. Electron-hole separation of a confined exciton in a square box ($w=0$, 2, and 5 nm as indicated). The solid (dashed) curves are for excitons with heavy (light) in-plane hole mass.

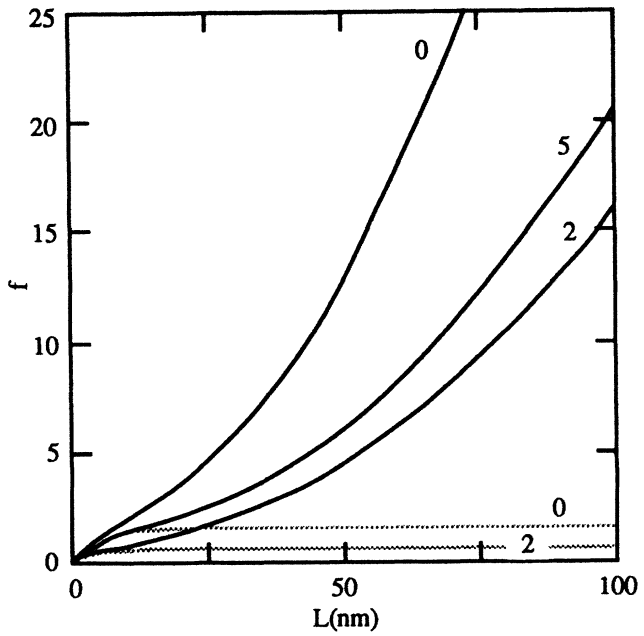

FIG. 10. Oscillator strength for the exciton confined in a square box ($w=0$, 2, and 5 nm as indicated). The solid curves are for correlated excitons. The dashed curves are for uncorrelated electron-hole pairs in the lowest-energy pair states. In all cases $m_{\perp,h}=0.377m$ and $m_{\parallel,h}=0.090m$.

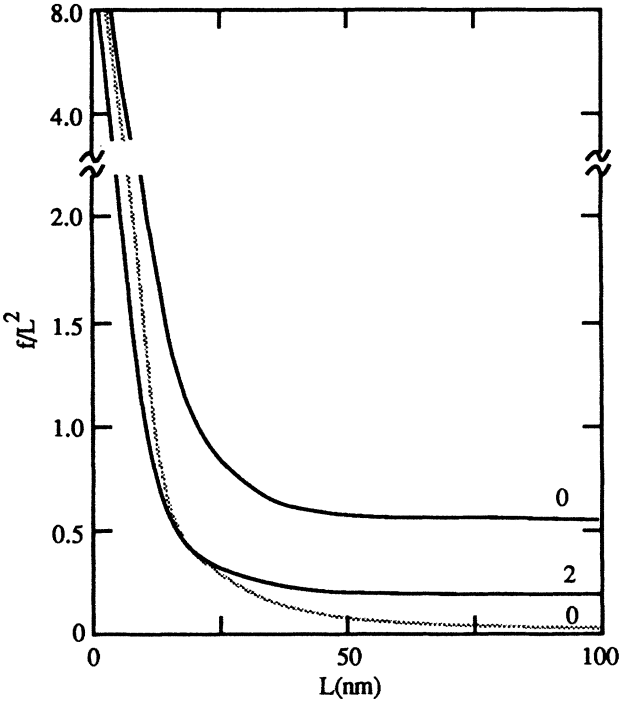

FIG. 11. Exciton oscillator strength normalized by the area L^2 of the box. The curves are the same as in Fig. 10.

ton confinement energy varies as $1/L^2$. Thus as L decreases, the energy denominator increases and f vanishes. Similarly, the exciton confinement energy for motion in the well varies as $1/w^2$; thus f decreases as w decreases. However, no confinement energy for z motion is included in E when $w=0$, so $f(w=0)$ is actually larger than $f(w\neq 0)$.

For large boxes the energy denominator is weakly dependent on L, so the integral of $\Psi(\mathbf{r}_e,\mathbf{r}_e)$ determines the behavior of f. Because of the difference in wave functions, the oscillator strength for an exciton in the fully correlated ground-state $f_{\rm ex}$ is very different from the oscillator strength f_p for an uncorrelated electron-hole pair in the lowest-energy pair state. The two oscillator strengths are compared in Fig. 10. For the two-dimensional ($w=0$) exciton,

$$\Psi(\mathbf{r}_e,\mathbf{r}_e)\sim 1/\sqrt{A A_{\rm ex}}\ ,$$

where $A=L^2$ is the two-dimensional area of the disk and $A_{\rm ex}$ is the area of the exciton. Consequently,

$$\left|\int \Psi(\mathbf{r}_e,\mathbf{r}_e)d^2r_e\right|^2\sim L^2/A_{\rm ex}\ .$$

For a fully correlated exciton, the oscillator strength is calculated from the coherent superposition of the amplitudes for absorbing a photon in each unit cell. Thus $f_{\rm ex}$ increases as L^2. For the uncorrelated two-dimensional ($w=0$) electron-hole pair

$$\Psi(\mathbf{r}_e,\mathbf{r}_e)=\frac{4}{L^2}\cos^2(kx_e)\cos^2(ky_e)$$

and $\int \Psi(\mathbf{r}_e,\mathbf{r}_e)d^2r_e=1$. Consequently, f_p is independent of L for large L. For $L^2\gg A_{\rm ex}$, $f_{\rm ex}$ is larger than f_p. For $L^2\lesssim A_{\rm ex}$, the exciton, if it were unaffected by confinement, would have an oscillator strength comparable to f_p. However, box confinement greatly weakens the correlation effects in the exciton. Thus for large L, $f_{\rm ex}$ is determined by the coherent superposition of transitions in each unit cell; for small L, $f_{\rm ex}$ converges to f_p because the pair becomes uncorrelated.

The oscillator strength is often normalized by the number of unit cells (sites, molecules, etc.) in the sample to give an oscillator strength per unit cell. Figure 11 shows f normalized by the area of the disk. For large L, $f_{\rm ex}/L^2$ is independent of L since $f_{\rm ex}$ is the coherent superposition of transitions in each unit cell. For small L, there is a strong enhancement of the normalized f. This occurs for L where correlation effects are weak and $f_{\rm ex}$ is converging to f_p. The enhancement in f is due to the increased electron-hole overlap that arises from the box confinement and is not due to coherent superposition effects.

This large enhancement in f/L^2 in the limit of complete quantum confinement has motivated others to suggest that quantum boxes should have enhanced optoelectronic properties.[19,20] However, there is substantial enhancement in f/L^2 even for $L\gtrsim 10$ nm. Thus quantum boxes which are not in the limit of complete quantum confinement may also provide enhanced optoelectronic properties.

Recent photoluminescence excitation measurements on quantum disks have revealed an enhanced luminescence efficiency. Kash *et al.*[5] suggested that the enhancement could arise from an increase in the radiative recombina-

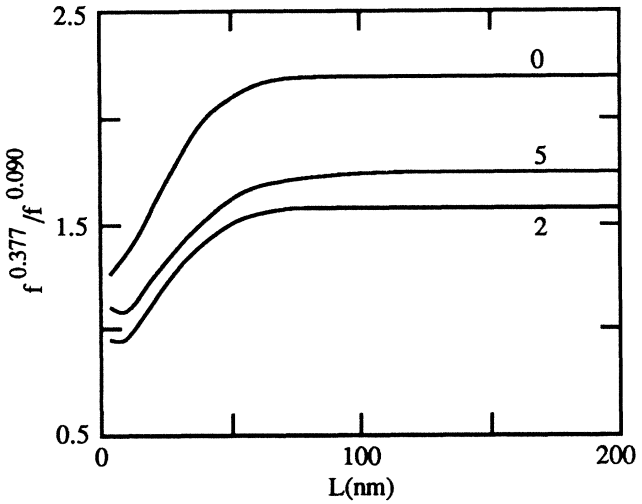

FIG. 12. Ratio of oscillator strengths for confined excitons with heavy and light in-plane hole masses. The w values are indicated.

tion rate of the lowest-energy exciton, an increase in the rates for scattering of carriers to band minima, or a decrease in nonradiative-recombination rates. They dismiss the first explanation by claiming that the structures are too large ($L \sim 50$ nm) for confinement effects to enhance recombination rates. In Fig. 12 we compare the oscillator strengths $f^{0.377}$ and $f^{0.090}$ for excitons with heavy and light in-plane hole masses. For $L \lesssim 100$ nm, we see an enhancement of $f^{0.090}$ relative to $f^{0.377}$. This occurs because confinement effects, which cause the enhancement of f, are more important for the exciton with the light in-plane hole mass. Since this exciton is the lower-energy exciton, confinement effects do increase the relative recombination rates of the lowest-energy exciton even for $L \approx 100$ nm. Thus this mechanism cannot be discounted as a cause of the enhanced photoluminescence efficiency.

IV. CONCLUSIONS

Confining an electron and a hole in a quantum box increases their direct Coulomb interaction because the two particles are constrained to occupy the same space despite any cost of increased kinetic energy. However, enhancement of the direct Coulomb interaction does not necessarily imply that Coulomb effects will be more important. The importance of Coulomb effects is determined by the extent to which the electron and hole can correlate in forming an exciton. Single-particle energy levels scale as $1/L^2$ and Coulomb energies scale as $1/L$. Thus confinement effects should become dominant as a box shrinks, and the electron-hole pairs will become uncorrelated despite the enhancement of the direct Coulomb interaction as the box shrinks. For square, GaAs quantum boxes, confinement effects become important when $L \sim 100$ nm. At this length scale the box is an order of magnitude larger than the free exciton. The single-particle, quantum-box energy levels can shift significantly as L changes, even when $L \gtrsim 100$ nm. However, these energies and the splittings between these levels are still much smaller than the free-exciton kinetic and Coulomb energies when $L \gtrsim 100$ nm. Consequently, confinement has little effect on the exciton for $L \gtrsim 100$ nm. For $L \approx 100$ nm, the confinement energies become comparable to the exciton energies and the Coulomb interactions become less effective at mixing single-particle states to form a correlated exciton. The transition to complete quantum confinement occurs when $L \lesssim 10$ nm. At this length scale, the box and exciton are the same size, the exciton energy is dominated by confinement energies, and there is no level mixing so the electron-hole pair occupy the pair of lowest-energy, single-particle states.

As the boxes shrink there is a larger reduction in electron-hole separation and an enhancement of the exciton oscillator strength. These are confinement effects, not effects due to the increase in direct Coulomb interaction induced by the confinement. In fact, the electron-hole separation determined solely with the correlated part of the exciton wave function increases as the box shrinks, indicating that correlation effects are becoming less important. Similarly, the enhanced confined-exciton oscillator strength is greater than the oscillator strength of a fully correlated, bulklike exciton. The enhancement is a confinement effect because the electron-hole pair becomes uncorrelated as the box shrinks.

The enhancement of the oscillator strength as L decreases can be significant even for L not in the regime of complete quantum confinement. The observed increase in luminescence efficiency in photoluminescence excitation measurements (for $L \sim 50$ nm) may result in part from the increase in the oscillator strength for the lowest-energy exciton relative to the oscillator strengths for other excitons. Calculations show that this increase occurs for $L \lesssim 100$ nm. Since the exciton oscillator strengths are enhanced for boxes which are larger than the limit for complete quantum confinement, these quantum boxes may possess the enhanced optoelectronics properties previously predicted for boxes which are in the complete confinement limit.

ACKNOWLEDGMENT

This research was conducted under the McDonnell Douglas Independent Research and Development program.

[1]P. M. Petroff, A. C. Gossard, R. A. Logan, and W. Wiegmann, Appl. Phys. Lett. **41**, 635 (1982).

[2]P. M. Petroff, J. Cibert, A. C. Gossard, G. J. Dolan, and C. W. Tu, J. Vac. Sci. Technol. B **5**, 1204 (1987).

[3]J. Cibert, P. M. Petroff, G. J. Dolan, S. J. Pearton, A. C. Gossard, and J. H. English, Appl. Phys. Lett. **49**, 1275 (1986).

[4]H. Temkin, G. J. Dolan, M. B. Panish, and S. N. G. Chu, Appl. Phys. Lett. **50**, 413 (1987).

[5]K. Kash, A. Scherer, J. M. Worlock, H. G. Craighead, and M. C. Tamargo, Appl. Phys. Lett. **49**, 1043 (1986).

[6]M. A. Reed, R. T. Bate, K. Bradshaw, W. M. Duncan, W. R. Frensley, J. W. Lee, and H. D. Shih, J. Vac. Sci. Technol. B **4**, 358 (1986).

[7]Y. Miyamoto, M. Cao, Y. Shingai, K. Furuya, Y. Suematsu, K. G. Ravikumar, and S. Arai, Jpn. J. Appl. Phys. **26**, L225 (1987).

[8]L. Brus, IEEE J. Quantum Electron. **QE-22**, 1909 (1986), and references therein.

[9]C. J. Sandroff, D. M. Hwang, and W. M. Chung, Phys. Rev. B **33**, 5953 (1986).

[10]J. Warnock and D. D. Awschalom, Appl. Phys. Lett. **48**, 425 (1986).

[11]A. I. Ekimov, A. A. Onushchenko, M. É. Raikh, and Al. L. Éfros, Zh. Eksp. Teor. Fiz. **90**, 1795 (1986) [Sov. Phys.—JETP **63**, 1054 (1986)].

[12]A. I. Ekimov, A. A. Onushchenko, S. K. Shumilov, and Al. L. Éfros, Pis'ma Zh. Tekh. Fiz. **13**, 281 (1987) [Sov. Tech. Phys. Lett. **13**, 115 (1987)].

[13]Y. Kayanuma, Solid State Commun. **59**, 405 (1986).

[14]H. M. Schmidt and H. Weller, Chem. Phys. Lett. **129**, 615 (1986).

[15]S. V. Nair, S. Sinha, and K. C. Rustagi, Phys. Rev. B **35**, 4098 (1987).

[16]L. E. Brus, J. Chem. Phys. **80**, 4403 (1984).

[17]Preliminary reports of this work have been given in G. W. Bryant, Surf. Sci. **196**, 596 (1988) and G. W. Bryant, in *Interfaces, Quantum Wells, and Superlattices,* edited by R. Taylor and E. W. Fenton (Plenum, New York, in press); see also T. Takejahara, Surf. Sci. **196**, 590 (1988).

[18]W.-Y. Wu, J. N. Schulman, T. Y. Hsu, and U. Efron, Appl. Phys. Lett. **51**, 710 (1987).

[19]M. Asada, Y. Miyamoto, and Y. Suematsu, IEEE J. Quantum Electron. **QE-22**, 1915 (1986).

[20]S. Schmitt-Rink, D. A. B. Miller, and D. S. Chemla, Phys. Rev. B **35**, 8113 (1987).

[21]G. W. Bryant, Phys. Rev. B **31**, 7812 (1985).

[22]G. W. Bryant, Phys. Rev. B **29**, 6632 (1984).

[23]G. Bastard, E. E. Mendez, L. L. Chang, and L. Esaki, Phys. Rev. B **26**, 1974 (1982).

[24]A configuration-interaction approach was used previously to calculate the electronic structure of multielectron systems in quantum boxes: G. W. Bryant, Phys. Rev. Lett. **59**, 1140 (1987); G. W. Bryant, D. B. Murray, and A. H. MacDonald, Superlatt. Microstruct. **3**, 211 (1987).

[25]H. A. Bethe and E. E. Saltpeter, *Quantum Mechanics of One- and Two-Electron Atoms* (Springer-Verlag, Berlin, 1957), p. 255.

[26]For example, É. I. Rashba and G. É. Gurgenishvili, Fiz. Tverd. Tela (Leningrad) **4**, 1029 (1962) [Sov. Phys.—Solid State **4**, 759 (1962)] and C. H. Henry and K. Nassau, Phys. Rev. B **1**, 1628 (1970).

[27]Y. C. Chiang and J. N. Schulman, Phys. Rev. B **31**, 2069 (1985).

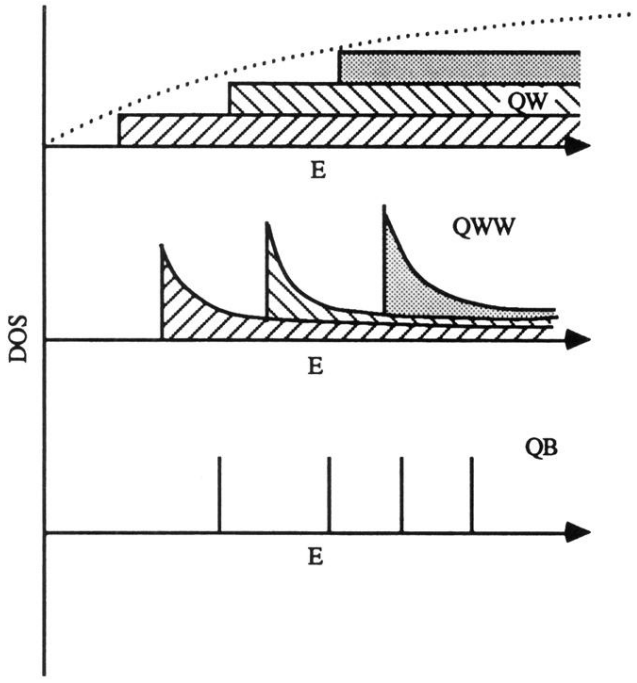

FIG. 1. The electronic density of states (DOS) for systems confined in one (quantum well), two (quantum-well wire) and three (quantum box) dimensions. The dashed line is the DOS for a bulk system.